Liquid Crystals
Publication details, including instructions for authors and subscription information:
http://www.informaworld.com/smpp/title~content=t713926090

Determination of the helical pitch in the smectic C*α phase by means of gyrotropy measurements

J. Ortega[a]; C. L. Folcia[b]; J. Etxebarria[b]; M. B. Ros[c]
[a] Departamento de Física Aplicada II. Facultad de Ciencias, Universidad del País Vasco, Apartado 644, 48080 Bilbao, Spain, [b] Departamento de Física de la Materia Condensada. Facultad de Ciencias, Universidad del País Vasco, Apartado 644, 48080 Bilbao, Spain, [c] Departamento de Química Orgánica. Facultad de Ciencias, Universidad de Zaragoza, 50009 Zaragoza, Spain,

Online publication date: 11 November 2010

To cite this Article Ortega, J. , Folcia, C. L. , Etxebarria, J. and Ros, M. B.(2003) 'Determination of the helical pitch in the smectic C*α phase by means of gyrotropy measurements', Liquid Crystals, 30: 1, 109 — 115
To link to this Article: DOI: 10.1080/0267829021000051755
URL: http://dx.doi.org/10.1080/0267829021000051755

LIQUID CRYSTALS, 2003, VOL. 30, NO. 1, 109–115

Determination of the helical pitch in the smectic C^*_α phase by means of gyrotropy measurements

J. ORTEGA
Departamento de Física Aplicada II. Facultad de Ciencias,
Universidad del País Vasco, Apartado 644, 48080 Bilbao, Spain

C. L. FOLCIA, J. ETXEBARRIA*
Departamento de Física de la Materia Condensada. Facultad de Ciencias,
Universidad del País Vasco, Apartado 644, 48080 Bilbao, Spain

and M. B. ROS
Departamento de Química Orgánica. Facultad de Ciencias,
Universidad de Zaragoza, 50009 Zaragoza, Spain

(*Received 15 May 2002; in final form 10 September 2002; accepted 19 September 2002*)

The existence of a short pitch helical structure in the smectic C^*_α phase has been confirmed in two compounds. This conclusion has been reached by using optical activity measurements along the helix axis and along a direction perpendicular to it. No measurable gyrotropy is detected along the helix, in agreement with earlier results. However, a rather large optical activity appears in the perpendicular direction. This optical rotation is difficult to detect, because it coexists with birefringence, and their separation requires the use of non-standard polarimetric techniques. The optical activity data, together with additional birefringence measurements performed simultaneously, have allowed us to obtain the helical pitch and the molecular tilt of the materials. The pitch is in the range 80–40 nm in the compounds studied, and its variation with temperature shows some irreproducible features on heating. On cooling from the smectic A phase, however, the pitch behaviour is perfectly reproducible.

1. Introduction

The smectic C^*_α (SmC^*_α) phase is one of the subphases normally exhibited by antiferroelectric liquid crystal materials. It appears usually between the SmA and the ferroelectric SmC*, or sometimes between the SmA and the ferrielectric SmC^*_{FI2} or the antiferroelectric SmC^*_A phase. SmC^*_α is a tilted phase with a small tilt angle θ which increases with decreasing temperature. In spite of the tilt, the phase is uniaxial and it is not easy to distinguish optically SmC^*_α from SmA.

Several structural models have been proposed in the literature for the SmC^*_α phase. The most recent experimental data [1–4] indicate a helical director structure with a very short pitch, at least when the sample is a free-standing film. When the material is inside a sandwich-type glass cell there is still some controversy. On the one hand, circular dichroism [5] and light scattering measurements [6] support a model consisting of a dynamical helical structure with a long average pitch. On the other hand, direct optical observations of Friedel fringes at the free surface of very flat drops [7] seem to ratify the short pitch model, although the relation between the helicity and the period of the observed fringes is not always obvious.

The aim of this work is to confirm the existence of the short pitch structure and obtain data for the helical pitch by using optical activity (OA) measurements in the SmC^*_α phase. Up to now, the OA of the SmC^*_α phase has always been measured along the normal to the smectic layers, where there is no birefringence. However, in this direction all the reported OA data have given null results [8–12]. This can be explained by the fact that the periodicity of the azimuthal angle is very small. Consequently, the SmC^*_α phase is uniaxial not only macroscopically, but even at the mesoscopic scale, thus hindering the OA along the helix axis. Here, however, we will present measurements along a direction different from the helix axis, where we have the advantage that the OA is quite large. This is at least the prediction of the so-called homogeneous optical model for short pitch

*Author for correspondence; e-mail: wmpetecj@lg.ehu.es

Liquid Crystals ISSN 0267-8292 print/ISSN 1366-5855 online © 2003 Taylor & Francis Ltd
http://www.tandf.co.uk/journals
DOI: 10.1080/0267829021000051755

materials reported in references [13–15]. Within the framework of this model it can be shown that if the pitch is much smaller than the light wavelength, the OA along a direction normal to the helix axis is several orders of magnitude larger than along the helix axis. OA measurements in this direction can then be used to test the existence of a short pitch in the SmC^*_α phase. Evidently, the measurements are not easy to perform, since the OA coexists with birefringence and these two quantities must be separated. Therefore, it is necessary to resort to non-standard polarimetric techniques.

This paper is organized as follows. In § 2 we briefly review the optical model used to interpret the measurements, giving the expressions for the OA along an arbitrary direction. The experiment is described in § 3 and the results and their analysis are presented in § 4 and 5. Finally we draw our conclusions.

2. OA in short pitch helical structures

Consider a helical structure with molecular director **n**, whose components are

$$n_x = \sin\theta\cos\varphi(z), \quad n_y = \sin\theta\sin\varphi(z), \quad n_z = \cos\theta. \tag{1}$$

Here $\varphi(z) = qz + \varphi_0$ is the azimuthal angle of the director, $q = 2\pi/p$ and p is the helical pitch. We will assume that the material is locally uniaxial, with ε_o and ε_e the principal values of the local dielectric tensor, which is given by

$$\varepsilon_{ij} = \varepsilon_o \delta_{ij} + \varepsilon_a n_i n_j \tag{2}$$

where $\varepsilon_a = \varepsilon_e - \varepsilon_o$ is the dielectric anisotropy.

It can be shown that for p much smaller than the optical wavelength λ (in practice for $\lambda > 5p$), a material defined by equation (2) behaves approximately as a homogeneous optically active uniaxial medium [13]. This can be demonstrated by using a perturbative approach based on the Berreman formalism [16] which rapidly converges when $p \ll \lambda$. Equation (2) defines our optical model for the SmC^*_α phase.

The main results of the above analysis are the following. The optic axis coincides with the z axis, and the principal values of the effective dielectric tensor (the squares of the main refractive indices) are

$$\tilde{\varepsilon}_o = \varepsilon_o(1 + \varepsilon_e/\tilde{\varepsilon}_e)/2, \quad \tilde{\varepsilon}_e = \varepsilon_o + \varepsilon_a\cos^2\theta. \tag{3}$$

On the other hand, the gyration tensor has two non-null elements up to first order in p/λ,

$$g_{xx} = g_{yy} = -\frac{p}{\lambda}\frac{\varepsilon_a^2}{8\tilde{\varepsilon}_e}\sin^2 2\theta \tag{4}$$

which means there is OA in a direction perpendicular to the optic axis (of magnitude $g_\perp = g_{xx}$), but not along the helix axis, i.e. $g_{zz} = g_\parallel = 0$. At first sight this may appear unexpected since, as is well known, that the de Vries equation predicts $g_\parallel \neq 0$, namely [10]

$$g_\parallel = -\frac{2\lambda}{p}\frac{\alpha^2}{8\lambda'^2(1-\lambda'^2)} \tag{5}$$

with

$$\lambda'^2 = \frac{2\lambda^2}{p^2(\varepsilon_\parallel + \varepsilon_o)}, \quad \alpha = \frac{(\varepsilon_\parallel - \varepsilon_o)}{(\varepsilon_\parallel + \varepsilon_o)}, \quad \frac{1}{\varepsilon_\parallel} = \frac{\sin^2\theta}{\varepsilon_e} + \frac{\cos^2\theta}{\varepsilon_o}. \tag{6}$$

However, as can be seen from equation (5), $g_\parallel$ scales as $(p/\lambda)^3$ for small p, vanishing for all practical purposes for $\lambda > 5p$. Therefore, for an arbitrary illumination direction making an angle β with the helix axis, the OA is simply

$$G = g_\perp \sin^2\beta + O(p^3/\lambda^3). \tag{7}$$

An estimate of orders of magnitude is highly illustrative. Consider a material with $\theta = 15°$, $p = 0.1\,\mu m$, $\varepsilon_o = 2.25$, and $\varepsilon_e = 2.72$. If we take $\lambda = 633\,nm$, equations (4) and (5) yield $g_\perp = -3.25 \times 10^{-3}$ and $g_\parallel = 1.77 \times 10^{-7}$, respectively. As can be seen, the OA along the helix axis is negligible (it corresponds to a rotatory power $\rho = 0.05°\,mm^{-1}$). However the gyration is huge in a perpendicular direction. In the absence of birefringence, this value of $g_\perp$ would correspond to a rotation angle per unit length ($\rho = \pi g_\perp/\lambda$) $\rho = -923°\,mm^{-1}$. The reason why these rotations are not usually observed is that the modifications in the polarization state of the light due to the OA are just small corrections to the main birefringence effects when both properties coexist. To separate the two effects, non-standard polarimetric techniques should inevitably be used.

3. Experimental procedure

As has been mentioned above, OA is extremely difficult to detect along birefringent crystal sections, and its effects can often be confused with those due to imperfections of the optical measuring system and sample surface defects. We have solved this difficulty by using the so-called high accuracy universal polarimeter (HAUP) technique [17]. The HAUP method permits us to control possible imperfections of the optical equipment, and to measure reliably the values of the birefringence, the OA and the indicatrix rotation when all these effects appear simultaneously. Basically, the experimental procedure consists in detecting the light intensity of a He-Ne laser after passing through a polarizer, the sample and an analyser for different polarizer angles. The angular displacements of polarizer and analyser are small (about 0.1°) and take place around the position of minimal transmission.

Typically, about 100 data points (intensity, polarizer angle, analyser angle) are taken for each temperature. The fit of these data to a theoretically derived function permits determination of the optical properties of the material. Figure 1 shows a scheme of the HAUP set-up. The most critical components of the equipment are two motorized, high quality polarizers that are rotated during the measurements with high accuracy and reproducibility (0.001° in our case). Although most of the studies with the HAUP method have been made on solid samples, the technique has already been applied to liquid crystal materials [18, 19]. The technical details of the apparatus and the experimental procedure can be found in reference [20].

We have studied two materials. The first one, ICOOET, was characterized using polarization measurements and broadband dielectric spectroscopy [21]. According to that work the phase sequence is

$$\text{SmA} \rightarrow (48^\circ\text{C})\ \text{SmC}^*_\alpha \rightarrow (41.8^\circ\text{C})\ \text{SmC}^*_{1/4} \rightarrow (32^\circ\text{C})\ \text{SmC}^*_{1/3} \rightarrow (27.7^\circ\text{C})\ \text{SmC}^*_\text{A}.$$

The second material is the well-known compound MHPOBC, which presents a SmC^*_α phase between a SmC* and a SmA according to the scheme

$$\text{SmA} \rightarrow (121.2^\circ\text{C})\ \text{SmC}^*_\alpha \rightarrow (119.2^\circ\text{C})\ \text{SmC}^* \rightarrow (118.4^\circ\text{C})\ \text{SmC}^*_{1/3} \rightarrow (117.4^\circ\text{C})\ \text{SmC}^*_\text{A}.$$

Glass cells coated with lecithin (hexadecyltrimethylammonium bromide, HTAB) to promote homeotropic alignment were used. The sample thickness was $L = 6\,\mu\text{m}$. The alignment was excellent in all phases except in the ferrielectric $SmC^*_{1/3}$ (i.e. SmC^*_{FI1} or SmC^*_γ) and $SmC^*_{1/4}$ (i.e. SmC^*_{FI2} or AF) phases, where domains with moving borders were observed. However, the order was recovered when exiting the ferrielectric phases both on heating and cooling. In contrast, the quality of planar cells, which seem more appropriate to measure $g_\perp$, was poorer and this type of cell was not used in our study.

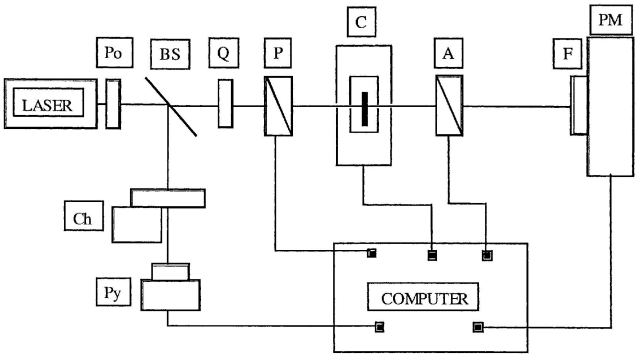

Figure 1. Block diagram of the HAUP set-up. The meaning of the symbols is the following. Po: polarizer, BS: beam splitter, Q: quarter-wave plate, P: prism polarizer, C: cryostat, A: prism analyser, F: interference filter for the laser wavelength, PM: photomultiplier, Ch: mechanical chopper, and Py: pyroelectric detector.

To measure $g_\perp$ the homeotropic cells were illuminated at an oblique incidence of 20°. This corresponds to an angle $\beta = 13^\circ$ between the layer normal and the illumination direction inside the material. The light source was a stabilized He-Ne laser with wavelength $\lambda = 632.8\,\text{nm}$. The material parameters directly determined from the experiment are the optical retardation Δ and the ellipticity of the normal modes k. These quantities are related to the birefringence $\Delta\tilde{n} \approx (\sqrt{\tilde{\varepsilon}_\text{e}} - \sqrt{\tilde{\varepsilon}_\text{o}})\sin^2\beta$ and the OA G along the illumination direction according to

$$\Delta = \frac{2\pi}{\lambda}\Delta\tilde{n}d \tag{8}$$

$$k = \frac{G}{2\Delta\tilde{n}} \tag{9}$$

where $d = L/\cos\beta$ is the interaction length.

4. Experimental results

First we will present the results corresponding to ICOOET, which has a remarkable SmC^*_α range. We will restrict ourselves to show the data on cooling after having annealed the sample for about 12 h in the SmA phase. It must be pointed out that a somewhat different gyration behaviour was found for cooling and heating runs. In addition, some differences were also detected among the heating runs depending on the initial conditions and thermal history. At this moment the reason for this peculiar behaviour is not clear, but some possibilities will be indicated at the end of the paper. To make explicit the degree of reproducibility and the experimental error of our measurements we present the results obtained in two consecutive cooling runs performed under the above conditions.

The birefringence in the direction normal to the optic axis $\Delta n = (\sqrt{\tilde{\varepsilon}_\text{e}} - \sqrt{\tilde{\varepsilon}_\text{o}})$ is represented in figure 2. This was obtained from the Δ data using equation (8) and the approximate expression $\Delta n \approx \Delta\tilde{n}/\sin^2\beta$. Δn is almost constant in the SmA phase and decreases on lowering the temperature in the SmC^*_α phase. This decrease is due to the appearance of a molecular tilt. In fact, using equation (3), the tilt angle can be easily obtained. This quantity has been plotted in figure 3. The temperature dependence is classical and the size of the tilt ($\theta \leqslant 10^\circ$) in the SmC^*_α phase is similar to data deduced from other measuring techniques [8].

Using the HAUP device as a conventional polarimeter we tried to determine the OA along the helix axis. However, as expected, an essentially null result was obtained ($\rho < 1^\circ\,\text{mm}^{-1}$). In contrast, the OA in a direction perpendicular to the helix is rather different. $g_\perp$ values

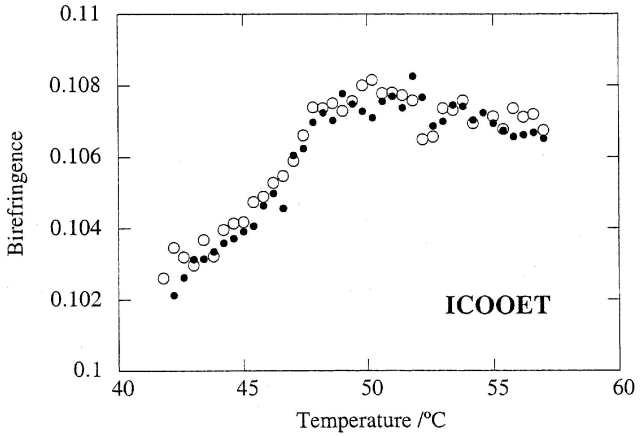

Figure 2. Temperature dependence of the birefringence of ICOOET around the SmA–SmC$^*_\alpha$ phase transition. Black and white circles correspond to two successive cooling runs.

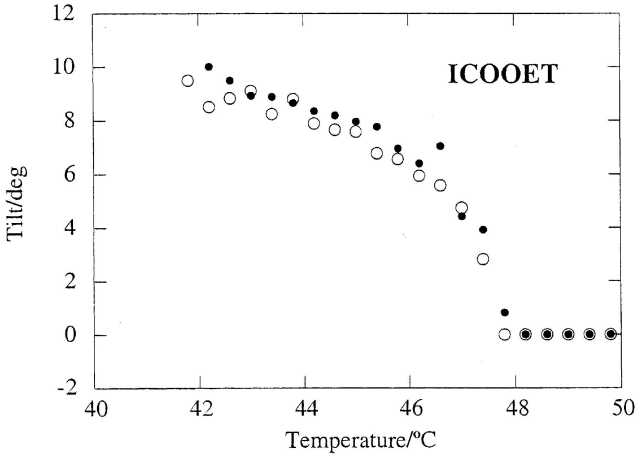

Figure 3. Temperature dependence of the molecular tilt angle of ICOOET as deduced from the birefringence data. Black and white circles have the same meaning as in figure 2.

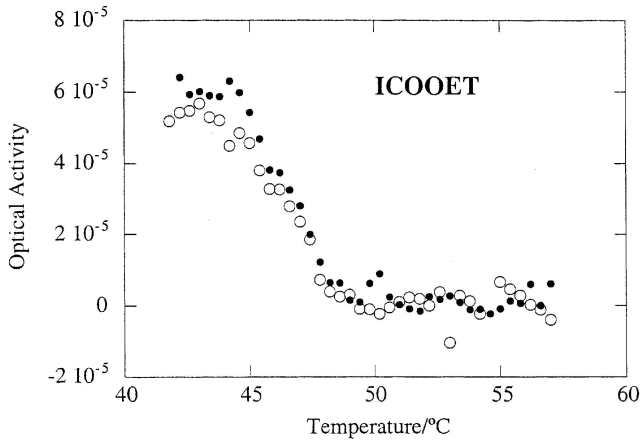

Figure 4. Temperature dependence of the gyration coefficient of ICOOET in a direction perpendicular to the helix axis. These values can be transformed into optical rotations per unit length by multiplying them by π/λ. Black and white circles have the same meaning as in figure 2.

are plotted in figure 4, and were deduced from the raw ellipticity k data by using equations (7–9). As can be seen, the SmA–SmC$^*_\alpha$ transition is easily observed. A clear non-null OA appears in the SmC$^*_\alpha$ phase, as predicted by the homogeneous optical model. It should be noted that these gyrations correspond to rather large optical rotations, about $\rho = 25^\circ\,\mathrm{mm}^{-1}$, as stated above.

Assuming the validity of the homogeneous optical model, the helical pitch can be deduced from $g_\perp$ by using equation (4). This quantity has been plotted in figure 5. It is practically constant in the SmC$^*_\alpha$ range, with values $p \sim 80\,\mathrm{nm}$. At high temperatures p is apparently larger, but in this region the experimental points are much scattered. These large errors are due to the lack of definition of the helix when the tilt is very small.

The results for MHPOBC are qualitatively similar. The temperature dependences of θ, $g_\perp$ and p are shown in figures 6, 7 and 8, respectively. In this material we could also determine the pitch in the SmC* phase below the SmC$^*_\alpha$ range, by using additional $g_\parallel$ data and equation (5). In figure 8, the last four points correspond to this phase and are in good accordance with earlier measurements [10]. In the SmC$^*_\alpha$ phase p is really small, $p \sim 40\,\mathrm{nm}$. Again, near the SmA phase the scattering of the data is remarkable and no reliable conclusion can be drawn.

5. Discussion and conclusions

The present measurements confirm the structural model of the short helical pitch for the SmC$^*_\alpha$ phase. This is in agreement with the results obtained on free-standing films by means of resonant X-ray scattering [1, 2] and ellipsometry [3, 4], and with the observations of Friedel fringes on flat drops [7]. Concerning the precise value of the pitch and its evolution with temperature, our results indicate that p is quite constant within the SmC$^*_\alpha$ phase, attaining small values (in the range of 50 nm) which depend on the material. In this respect, although there are still very few published data, we can say that there exists no universal behaviour for the evolution and magnitude of p in the SmC$^*_\alpha$ phase. For example, in references [1–3], it has been found that in the SmC$^*_\alpha$ phase of 10OTBBB1M7, p is extremely small (between 5 and 8 layers, about 20–30 nm) and increases with temperature. However, in 11HFBBM7, p is a decreasing function of temperature [4] and varies between 80 and 160 nm. In this sense, recently it has been found that small molecular changes produce dramatic effects in the pitch behaviour of SmC$^*_\alpha$ free-standing films [22]. On the other hand, in reference [7], rather complicated

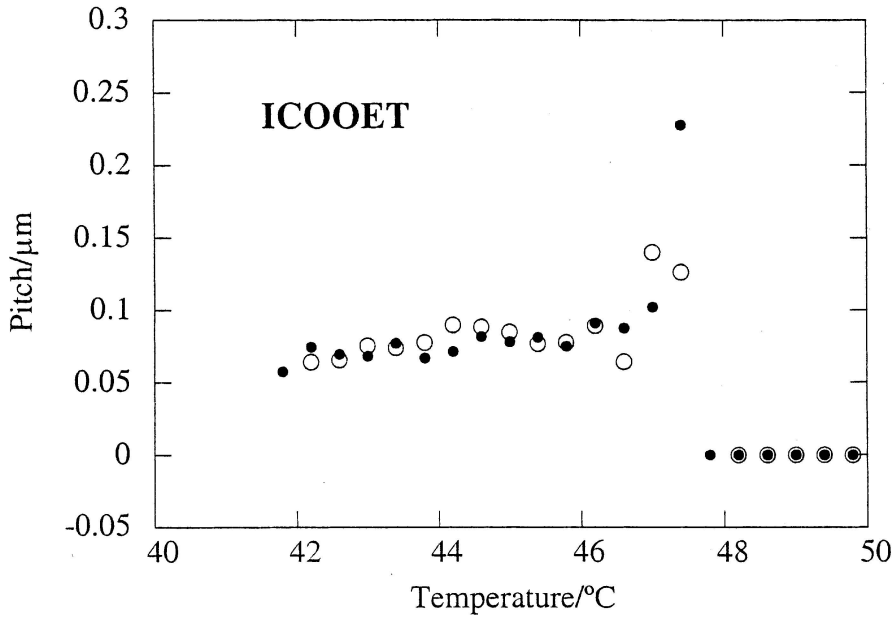

Figure 5. Temperature dependence of the helical pitch of ICOOET as deduced from the gyration perpendicular to the helix axis and the tilt angle assuming the validity of equation (4). Black and white circles have the same meaning as in figure 2.

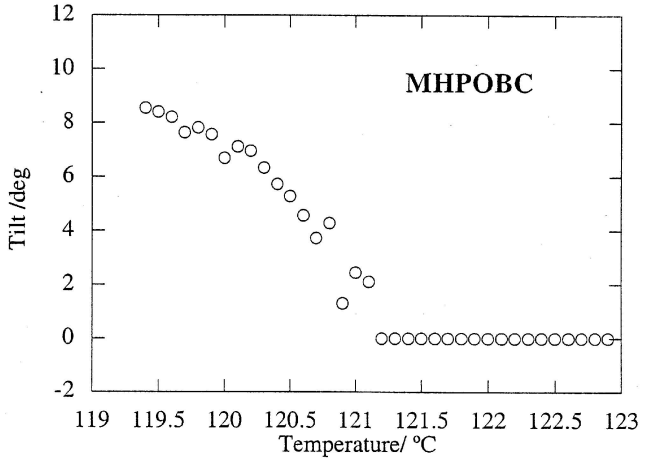

Figure 6. Temperature dependence of the molecular tilt angle of MHPOBC as deduced from the birefringence.

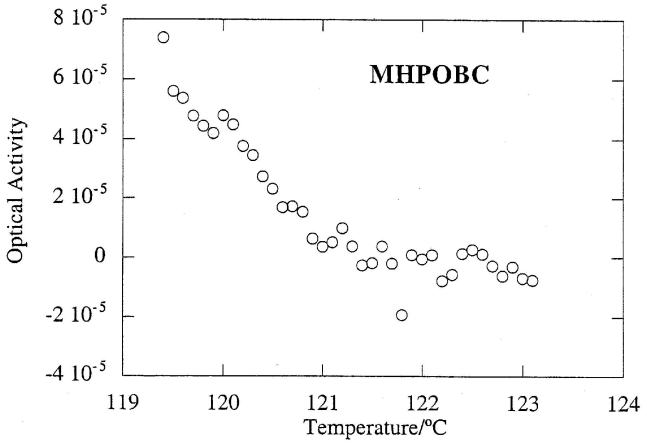

Figure 7. Temperature dependence of the gyration coefficient of MHPOBC in a direction perpendicular to the helix axis.

temperature dependences are reported for the double optical period of the Friedel ellipticity fringes (which are related to p) in the SmC^*_α phases of a thiobenzoate series.

It is also interesting to point out that although the experiments performed on free-standing films do not have problems of reproducibility [1–4], this is not the case with the behaviour of the Friedel fringes on drops. In fact, in reference [7] several scenarios are found for the evolution of the double optical period depending on the initial conditions. This lack of reproducibility is in agreement with our results, especially for ICOOET on heating. It seems that the helical structure of the SmC^*_α phase is very fragile and therefore depends strongly on the surface boundary conditions. The fragility can be due to the weakness of the azimuthal angular correlations, which are brought about by steric, van der Waals and electrostatic interactions combined in a rather complicated way [8]. Apart from the forces between nearest neighbours, at least next-nearest neighbour interactions appear to be important to explain the formation of a SmC^*_α phase. It is then reasonable to think that the balance between all these interactions is rather delicate and can be easily perturbed by small defects or imperfections, which are likely to be absent in freely suspended films, but not in confined samples.

Lastly, a question can be raised regarding the validity of the homogeneous optical model for an accurate description of the SmC^*_α phase. In the shortest pitch conditions ($p \sim 40\,\text{nm}$), the azimuthal angle φ of the director undergoes shifts between consecutive layers as

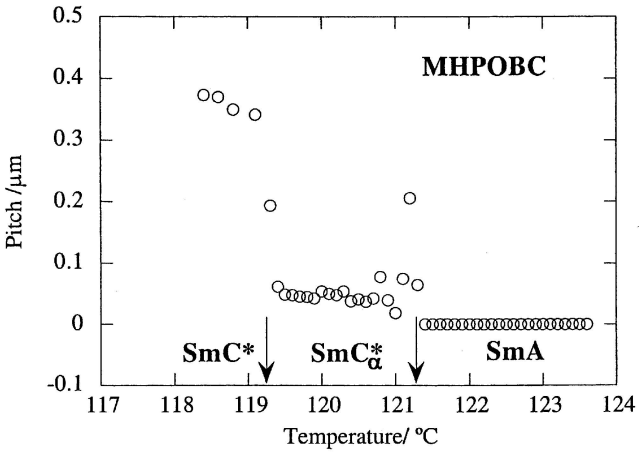

Figure 8. Temperature dependence of the helical pitch of MHPOBC as deduced from the gyration perpendicular to the helix axis and the tilt angle. The data below 119.2°C correspond to the SmC* phase and were derived from the OA along the helix axis using the de Vries formula.

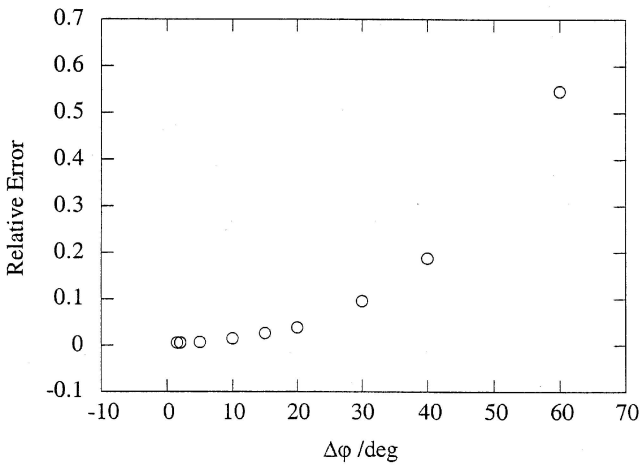

Figure 9. Comparison showing the relative error between the OA along the helix axis calculated with the assumption of a continuous azimuthal angle $\varphi(z)$, and the data obtained using the exact Berreman model. $\Delta\varphi$ in the abscissa axis is the change of the azimuthal angle of the director between adjacent smectic layers.

large as 30° (assuming a typical layer thickness around 3 nm). In this limit, $\varphi(z)$ is clearly a discrete function and in no way can be considered continuous, as the homogeneous model assumes [13–15]. Therefore, the suitability of the model in this extreme limit is not fully justified.

In order to clarify this point, a comparison between the gyrotropy predicted by the homogeneous model and that obtained by carrying out the exact calculation using the discrete Berreman formalism has been performed. Unfortunately, the determination of any homogeneous optical property using the Berreman formalism [16] is not evident in general directions and, in particular, the gyrotropy is only easily calculated along the optic axis. Therefore, we have restricted ourselves to comparing the exact $g_{\|}$ values with those deduced from a model in which φ is a continuous function of z. The latter is just the de Vries formula, equation (5). In any case, if the OA along the optic axis is correctly calculated by the de Vries theory, it seems reasonable to assume the validity of the continuous approach for $\varphi(z)$.

Figure 9 shows the relative error of the approximate calculation of the rotatory power using equation (5), taking as exact the result obtained with the Berreman method. As can be seen, below azimuthal angle shifts of 30° the error lies within an acceptable range (<10%). This result justifies the validity of the homogeneous optical model for the materials studied in the present work.

This work is supported by the CICYT of Spain (Project No. MAT2000-1293-C02) and the University of the Basque Country (Project No. 9/UPV 00060.310-13562/2001).

References

[1] Mach, P., Pindak, R., Levelut, A. M., Barois, P., Nguyen, H. T., Huang, C. C., and Furenlid, L., 1998, *Phys. Rev. Lett.*, **81,** 1015.
[2] Mach, P., Pindak, R., Levelut, A. M., Barois, P., Nguyen, H. T., Baltes, H., Hird, M., Toyne, K., Seed, A., Goodby, J. W., Huang, C. C., and Furenlid, L., 1999, *Phys Rev. E*, **60,** 6793.
[3] Johnson, P. M., Pankratz, S., Mach, P., Nguyen, H. T., and Huang, C. C., 1999, *Phys Rev. Lett.*, **83,** 4073.
[4] Schlauf, D., Bahr, Ch., and Nguyen, H. T., 1999, *Phys. Rev E*, **60,** 6816.
[5] Yamada, K., Takanishi, Y., Ishikawa, K., Takezoe, H., Fukuda, A., and Osipov, M. A., 1997, *Phys. Rev. E*, **56,** R43.
[6] Konovalov, D., and Sprunt, S., 1998, *Phys. Rev E*, **58,** 6869.
[7] Laux, V., Isaert, N., Joly, G., and Nguyen, H. T., 1999, *Liq. Cryst.*, **26,** 361.
[8] Skarabot, M., Cepic, M., Zeks, B., Blinc, R., Heppke, G., Kityk, A. V., and Musevic, I., 1998, *Phys. Rev E*, **58,** 575.
[9] Beaubois, F., Marcerou, J. P., Nguyen, H. T., and Rouillon, J. C., 2000, *Eur. Phys. J. E*, **3,** 273.
[10] Musevic, I., and Skarabot, M., 2001, *Phys. Rev. E*, **64,** 051706.
[11] Shtykov, N. M., Vij, J. K., and Nguyen, H. T., 2001, *Phys. Rev. E*, **63,** 051708.
[12] Akizuki, T., Miyachi, K., Takanishi, Y., Ishokawa, K., Takezoe, H., and Fukuda, A., 1999, *Jpn. J. appl. Phys.*, **38,** 4832.
[13] Oldano, C., and Rajteri, M., 1996, *Phys. Rev. B*, **54,** 10273.
[14] Hubert, P., Lägemalm, P., Oldano, C., and Rajteri, M., 1998, *Phys Rev E*, **58,** 3264.
[15] Galatola, P., 1997, *Phys. Rev. E*, **55,** 4338.

[16] Berreman, D. W., 1972, *J. opt. Soc. Am.*, **62,** 502.
[17] Kobayashi, J., and Uesu, Y., 1983, *J. appl. Crystallogr.*, **16,** 204.
[18] Ortega, J., Etxebarria, J., and Folcia, C. L., 2000, *Eur. Phys. J. E*, **3,** 21.
[19] Etxebarria, J., Folcia, C. L., and Ortega, J., 2001, *Phys. Rev. E*, **64,** 011707.
[20] Folcia, C. L., Ortega, J., and Etxebarria, J., 1999, *J. Phys. D*, **32,** 2266.
[21] Merino, S., de la Fuente, M. R., González, Y., Pérez Jubindo, M. A., Ros, B., and Puértolas, J. A., 1996, *Phys. Rev. E*, **54,** 5169.
[22] Cady, A., Olson, D. A., Han, X. F., Nguyen, H. T., and Huang, C. C., 2002, *Phys. Rev. E*, **65,** 030701.